

## CALIBRATION METHODS FOR EDDY CURRENT MEASUREMENT SYSTEMS\*

J. C. Moulder and J. C. Gerlitz

Fracture and Deformation Division  
National Bureau of Standards  
Boulder, Colorado 80303

B. A. Auld, M. Riaziat, S. Jeffries, and G. McFetridge

Edward L. Ginzton Laboratory  
Stanford University  
Stanford, California 94305

### INTRODUCTION

Calibration of eddy current measurement systems is an important factor for attaining the accuracy and precision of measurement that quantitative nondestructive evaluation requires. The quantity of interest in most forms of eddy current inspection is  $\Delta Z$ , the change in probe impedance induced by a flaw. Flaw signals produced by surface-breaking cracks are small; typical flaw signals for an air core probe amount to a few tenths of one percent of the probe's impedance in air. Such small signals are easily obscured by the impedance changes caused by small variations in the height of the probe above the workpiece (lift-off). To discriminate against lift-off, conventional eddy current instruments determine the phase of  $\Delta Z$  relative to lift-off and the magnitude of the component of  $\Delta Z$  in quadrature with lift-off. But this information is not sufficient to perform flaw signal inversion; rather, the absolute magnitude and phase of  $\Delta Z$  are necessary. Thus, quantitative inversion of eddy current signals to obtain flaw sizes requires methods for calibrating eddy current measurement systems.

To properly calibrate an eddy current probe, several possibilities exist: (1) comparison of experimental lift-off data with theory, (2) comparison of theoretical and experimental probe response to flaws that can be analyzed accurately, and (3) insertion of small resistances in series with the probe to provide fiducial marks on the response obtained for an unknown flaw. This paper describes the results of a study comparing all these methods. To facilitate comparisons of theory and experiment we used air core probes, for which the magnitude and spatial distribution of the magnetic field can be accurately calculated using the analysis of Dodd and Deeds (1968).

---

\*Contribution of the National Bureau of Standards, not subject to copyright.

## THEORY

The general problem of calculating the impedance of a rectangular cross-section, circular coil above a semi-infinite conductor has been solved analytically by Dodd and Deeds (1968) using a vector potential approach. The geometry of the problem to be considered here is illustrated in Fig. 1, which shows an air core coil of thickness  $t$ , width  $\Delta r$ , and mean radius  $\bar{r}$  located a distance  $h$  above an infinite plane of conductivity  $\sigma$  and permeability  $\mu$ . In what follows, we adopt the notation of Bahr and Cooley (1983) and normalize all dimensional quantities by dividing by  $\bar{r}$ . For a coil of  $N$  turns operating at an angular frequency  $\omega$ , Bahr and Cooley give an expression for the impedance of the test probe,  $Z_{TP}$ :

$$Z_{TP} = i\omega\mu \frac{\pi\bar{r}N^2}{(t\Delta r)^2} I_{TP}, \quad (1)$$

where probe current is given by

$$I_{TP} = \int_0^\infty \frac{I_\alpha^2}{\alpha^5} \left\{ 2t + \frac{1}{\alpha} \left[ 2(e^{-\alpha t} - 1) + e^{-2\alpha h} (e^{-\alpha t} - 1)^2 \left( \frac{\alpha - \alpha_1}{\alpha + \alpha_1} \right) \right] \right\} d\alpha \quad (2)$$

with

$$I_\alpha = \int_{\alpha(1 - \frac{\Delta r}{2})}^{\alpha(1 + \frac{\Delta r}{2})} u J_1(u) du \quad (3)$$

$$\alpha_1 = \sqrt{\alpha^2 + i2(\bar{r}/\delta)^2} \quad (4)$$

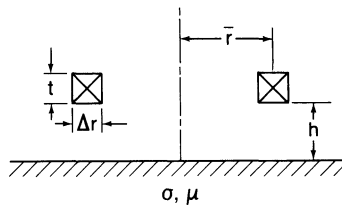


Fig. 1. Coil geometry for lift-off calculations.

In the expressions above,  $i = \sqrt{-1}$ ,  $\alpha$  and  $u$  are variables of integration,  $\delta$  is the electromagnetic skin depth, and  $J_1$  is the Bessel function of the first kind and first order. From equation (1), it is a simple matter to calculate the change in probe impedance  $\Delta Z_{LO}$  caused by a small change  $\Delta h$  in the height of the probe above the surface:

$$\Delta Z_{LO} = \left. \frac{dZ_{TP}}{dh} \right|_{h_0} \Delta h \tag{5}$$

where  $h_0$  is the initial lift-off height. Differentiating equation (1) with respect to  $h$  and substituting into equation (5) yields

$$\Delta Z_{LO} = i\omega\mu \frac{\Delta h \bar{r} N^2}{(t\Delta r)^2} I'_{TP} \tag{6}$$

where the derivative of probe current with respect to lift-off height is given by

$$I'_{TP} = - \int_0^\infty \left[ \frac{I_\alpha^2}{\alpha^5} 2e^{-2\alpha h_0} (e^{-\alpha t} - 1)^2 \left( \frac{\alpha - \alpha_1}{\alpha + \alpha_1} \right) \right] d\alpha. \tag{7}$$

Equations (6) and (7) permit the calculation of lift-off response for an arbitrary coil conforming to the geometry of Fig. 1. Note that  $\Delta Z_{LO}$  depends on frequency only according to the variables  $\omega$  and  $\bar{r}/\delta$ , the latter through the dependence of  $I'_{TP}$  on  $\alpha_1$ .

It is considerably more difficult to calculate probe impedance changes produced by flaws because of the greater geometrical complexity of a flaw compared to a smooth surface. Yet much progress has been made in recent years on quantitative modeling of probe field-flaw interactions, as delineated in the recent reviews by Auld et al. (1984 a and b). In particular, fully parametrized solutions for the response of an eddy current probe to a flaw are now available for the case of rectangular-shaped surface-breaking flaws interrogated by a nonuniform probe-field (Muennemann et al., 1983; Auld et al., 1984a). The assumptions of presently available models include a high-conductivity workpiece, flaw depth greater than skin depth ( $a/\delta > 2$ ), and flaw length greater than mean coil radius ( $2c > \bar{r}$ ). An additional requirement is that the field distribution of the probe be known, either by calculation or measurement (Auld et al., 1984c). The availability of such models points to the possibility of using artifact standards ("standard flaws") to calibrate eddy current measurement systems, a possibility we consider here. It should be emphasized, however, that this does not correspond to the common practice of maintaining a catalogue of flaw responses for particular types and sizes of flaws one wishes to detect. Instead, we envisage a procedure whereby the flaw signal obtained from a standard flaw by an uncalibrated eddy current measurement system is compared to the calculated flaw signal to achieve calibration. Obviously, such a procedure demands a high degree of confidence in the theoretical model used to calculate flaw responses. The comparisons of theory and experiment undertaken in this study are an important step in this direction.

Calculations of flaw signals for the flaws and probe used in this study were performed at Stanford University using the nonuniform-field probe-flaw interaction theory developed there (Muennemann et al., 1983; Auld et al., 1984a and b). These calculations are discussed in greater detail elsewhere in these proceedings (Auld et al., 1984d).

## EXPERIMENT

To provide a meaningful comparison of theory and experiment, a number of precautions were observed in the design and execution of the experiments. Air core probes were used to permit the field distribution and lift-off response to be calculated accurately using existing theory. For accurate and reproducible positioning of the probe relative to the flaw, a manual three-axis micropositioner was used for scanning the probe along the length of the flaw. The micropositioner was mounted on an optical table with the probe held in a vee block attached to the positioner. Flaw specimens were clamped to the optical table under the probe, with careful attention to alignment so that a constant lift-off could be maintained during flaw scans. Scanning was performed along the length of the flaw, with the probe centered on the flaw's axis; measurements were taken at 0.5-mm intervals. This mode of scanning produces a signature characteristic of the probe-flaw geometry and gives maximum sensitivity because the interruption of eddy currents by the flaw is maximized (Auld et al., 1984a). The eddy current probe used for lift-off and flaw-signal measurements was an absolute pencil probe with a 235-turn air core coil, designed for 200 kHz operation. Its physical dimensions were:  $r = 0.81$  mm,  $\Delta r = 1.22$  mm,  $t = 3.56$  mm, and  $h_0 = 0.51$  mm. This same probe was used in several earlier studies by other groups (Auld et al., 1984c; Muennemann et al., 1984; and Rummel and Rathke, 1984).

Another important consideration was the measurement system used to determine changes in probe impedance. We chose to use a precision commercial impedance analyzer that could directly determine probe impedance over a broad frequency range (5 Hz to 13 MHz). This instrument's impedance measuring function is based on the vector voltage/current ratio method, whereby the probe impedance is determined by measuring the vector ratio between the applied test signal voltage and the current flowing through the probe. To achieve a broad frequency range of operation, it employs an autobalance bridge circuit in the measurement section. The use of this instrument offers considerable advantages over conventional eddy current measurement systems using a bridge and amplifier, since the latter approach requires knowledge of the frequency dependence of the amplifier's transfer function (Bahr, 1982). For the measurements reported here, we estimate an overall uncertainty of  $\pm 0.32 \Omega$  in determining the magnitude of  $\Delta Z$  and  $\pm 14^\circ$  in determining the phase. The relatively large experimental uncertainty, comparable in magnitude to the flaw signals we wished to measure, arises because  $\Delta Z$  is determined by taking the vector difference of two nearly equal impedances. The precision of probe impedance measurements was much better:  $\pm 0.07 \Omega$  in magnitude and  $\pm 0.01^\circ$  in phase, estimated from the standard error determined for a series of independent measurements performed over a period of several days. Although the accuracy with which  $\Delta Z$  could be determined is only marginally adequate for comparing observation with theory, the reproducibility of the measurements was good. This fact suggests that a more sensitive instrument might be especially designed for eddy current measurements,

embodying the same measurement principles as this instrument, but sacrificing some of its range and versatility for greater sensitivity.

Flaw signal measurements were obtained for seven specimens: one fatigue crack in aluminum alloy 2024 and a series of six rectangular-shaped, electrical-discharge machined (EDM) notches in aluminum alloy 6061. Aluminum alloy specimens were used because a high-conductivity workpiece is assumed in the theoretical model. For brevity, we report here the results for only two flaws: the fatigue crack and one EDM notch. The fatigue crack we studied is 3.81 mm long (determined visually) and has an estimated depth of 1.27 mm. The EDM notch is 6.60 mm long, 0.56 mm deep, and 0.28 mm wide. These two specimens were also used for the lift-off-response measurements reported here.

A different measurement system was used to study the electrical calibration method of inserting small resistances in series with the probe. This system was composed of a broadband inductive bridge connected to two similar air core coils in a differential configuration, a calibration box containing a number of small resistances (0.01 - 5  $\Omega$ ) that could be switched into series connection with one of the coils, a signal source, and a lock-in amplifier equipped with independent magnitude and phase outputs to measure bridge output signals. The bridge was similar in design to one described previously (Muennemann et al., 1983), and could operate at frequencies of 0.1 - 1 MHz. Impedance values for each resistor in the calibration box were independently determined at the frequencies of interest using the aforementioned impedance analyzer.

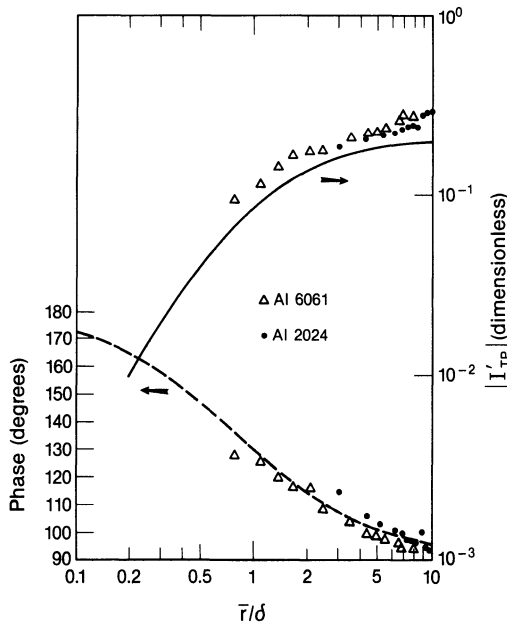


Fig. 2. Lift-off response of an air core probe compared to the response predicted by Equation (7).

## RESULTS AND DISCUSSION

Measurements of lift-off response for the absolute eddy current probe were performed for a fixed change in lift-off height ( $\Delta h = 0.074$  mm) on both specimens over a range of frequencies. The frequency was varied from 0.01 - 1.0 MHz for the Al 6061 specimen and from 0.1 - 1.0 MHz for the Al 2024 specimen. The results are compared to theoretical predictions in Fig. 2. The theoretical curves for  $I'_{TP}$  were calculated using Equation (7); experimental values for  $I'_{TP}$  were determined using Equation (6) and the measured values of  $\Delta Z_{LO}$ . Differences between prediction and observation are approximately 20% for the magnitude and 3% for the phase of  $I'_{TP}$ . These differences are well within the experimental uncertainty, confirming that lift-off measurements may be used with confidence to calibrate air core eddy current probes.

The results of flaw signal measurements at several frequencies for the EDM notch in Al 6061 are shown in Figs. 3 and 4, together with the theoretical predictions. In Fig. 3 the magnitude of  $\Delta Z$  is plotted against the position of the probe relative to the center of the flaw, normalized by  $r$ . Theoretical curves were adjusted by a fixed parameter, chosen to give agreement between theory and experiment at the center of the flaw at 550 kHz; this was done for clarity of presentation. Actual differences between theory and experiment for the magnitude of  $\Delta Z$  were approximately 25%, well within the experimental uncertainty but greater than the disagreement found for lift-off measurements. However, the qualitative agreement is excellent. Figure 4 shows experimental and theoretical results for the phase of  $\Delta Z$  for the same flaw. In this case no adjustments were made to the theoretical curves. Predicted and observed values for the phase of  $\Delta Z$  differed by about  $8^\circ$  at the center of the flaw. This difference is also within the bounds of experimental uncertainty, but greater than that observed for lift-off measurements. The noise that is evident in the experimental phase curves makes it difficult to assess the qualitative agreement with theory, but it appears that the structure exhibited by the theoretical curves is less pronounced in the experimental results. Furthermore, the observed phase drops more rapidly at the end of the flaw than theory predicts.

Measurements of the magnitude of  $\Delta Z$  for the fatigue crack are compared to theoretical predictions in Fig. 5. Once again, the theoretical curve was fitted to the experimental results at the center of the flaw for this figure, but the difference between observation and theory was within the experimental uncertainty. In performing the calculations for this specimen, the flaw was modeled as a rectangular-shaped crack with zero width (opening). The assumption of rectangular shape causes the model to predict higher impedance values at the ends of the crack than are observed. Since the fatigue crack is expected to have a semi-elliptical shape, and therefore a smaller depth at the ends of the crack than in the center, this result is not unexpected.

Electrical calibration of the inductive bridge circuit by inserting small resistances in series with the probe was studied at two frequencies: 500 kHz and 1 MHz. The results of this experiment are shown in Fig. 6, where the magnitude and phase of the change in bridge output voltage,  $\Delta V$ , are plotted against the magnitude and phase of the calibrating impedance. Values for the magnitude of  $\Delta V$  were normalized to the magnitude of the residual bridge imbalance signal with no calibration resistor in place. The solid lines in the figure show the results of linear regression analyses of the experimental data. The

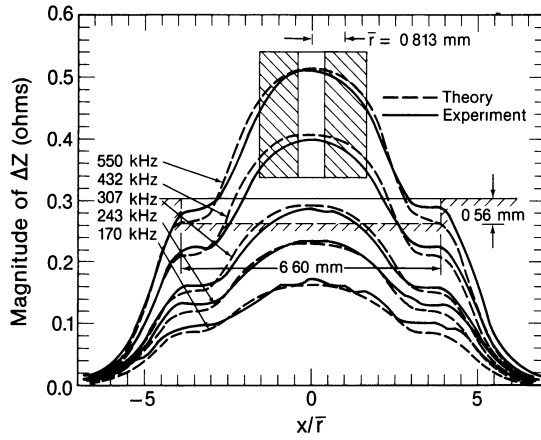


Fig. 3. Magnitude of  $\Delta Z$  determined by scanning the probe along the length of an EDM notch in Al 6061. Theoretical curves were calculated from the nonuniform-field probe-flaw interaction theory of Auld et al. (1984b). The abscissa represents normalized probe position relative to the center of the flaw.

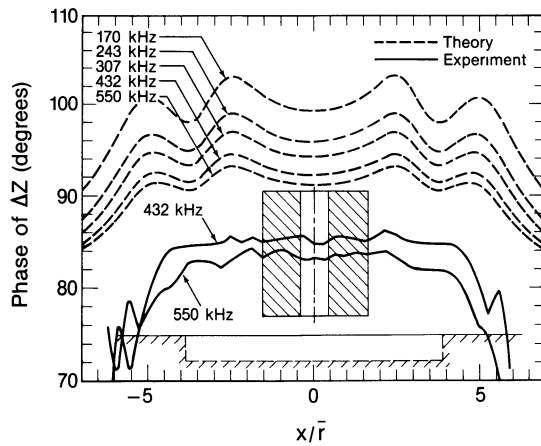


Fig. 4. Phase of  $\Delta Z$  for the same flaw shown in Fig. 3.

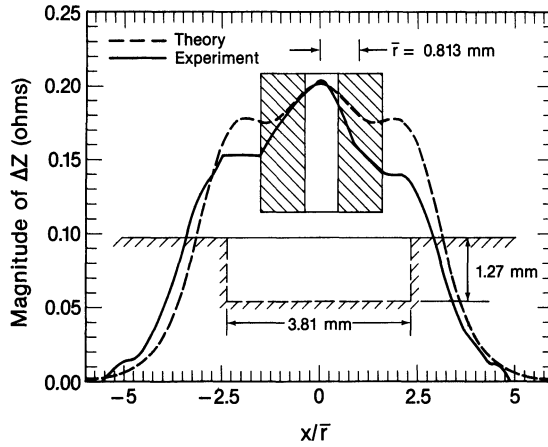


Fig. 5. Magnitude of  $\Delta Z$  determined for a probe scanned along the length of a fatigue crack in Al 2024. For theoretical calculations, the crack was modeled as a rectangular-shaped flaw.

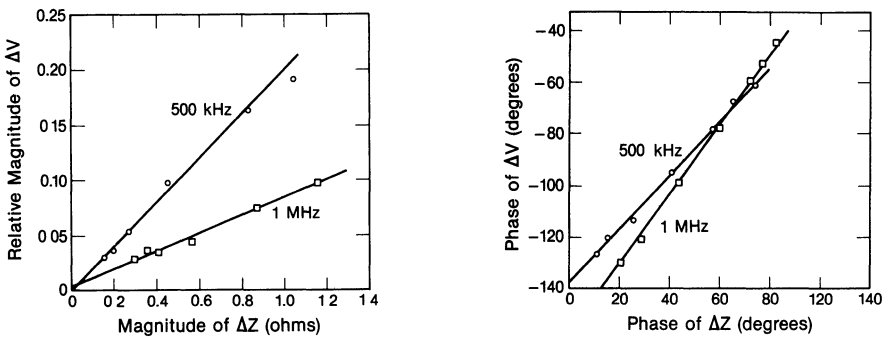


Fig. 6. Results of electrical calibration of an inductive bridge by inserting small resistances in series with the eddy current probe.



results illustrate that the response of the bridge is linear for impedance changes of up to  $1 \Omega$ , and that a small real impedance is capable of calibrating the entire eddy current measurement system in both magnitude and phase.

Although the electrical calibration technique requires that additional circuitry be incorporated into the eddy current measurement system, it does offer two significant advantages over the other two calibration methods we studied. First, electrical calibration may be used with either air core or ferrite core probes in either a differential or absolute probe configuration. Calibration methods based on comparing measurements of probe response to theoretical predictions require knowledge of the probe's magnetic field intensity and spatial distribution. This information can be calculated for air core probes using existing theory, but for ferrite core probes it would have to be obtained by additional measurements (Auld et al., 1984c). Second, the electrical calibration technique offers the possibility of in situ calibration: calibrating resistances could be switched into the circuit during the measurement process to provide fiducial marks on the response obtained for an unknown flaw.

## CONCLUSIONS

From this study of three different approaches to the calibration of eddy current measurement systems, the following conclusions emerge:

1. Insertion of small resistances in series with an eddy current probe calibrates the entire measurement system in both magnitude and phase. This method can be used for both air core and ferrite core probes.
2. Measurements of lift-off signals obtained with an air core probe were found to be in good agreement with the lift-off response calculated from the theory of Dodd and Deeds (1968).
3. Measurements of flaw signals for an EDM notch and a fatigue crack in aluminum alloy specimens were found to agree with the predictions of the nonuniform-field probe-flaw interaction theory of Auld et al. (1984b).
4. Extension of the latter two calibration methods to a ferrite core probe requires measurement of the probe's field strength and shape.

## ACKNOWLEDGMENTS

This work was supported by the National Bureau of Standards Office of Nondestructive Evaluation. W. Rummel and R. Schaller of Martin Marietta (Denver) kindly supplied the eddy current probe used in this study. Probe lift-off response was programmed and calculated at Stanford Research Institute by A. Bahr and D. Cooley. The fatigue crack specimen was produced by O. Buck while at Rockwell International.

## REFERENCES

- Auld, B. A., Ayter, S., Muennemann, F., and Riaziat, M., 1984a, Eddy current signal calculations for surface breaking cracks, in: "Review of Progress in Quantitative Nondestructive Evaluation 3," D. O. Thompson and D. E. Chimenti, eds., Plenum, New York and London.
- Auld, B. A., Muennemann, F., and Riaziat, M., 1984b, Quantitative modelling of flaw responses in eddy current testing, in: "Research Techniques in Nondestructive Testing, Vol. VII," R. S. Sharpe, ed., Academic, London.
- Auld, B. A., Muennemann, F. G., and Burkhardt, G. L., 1984c, Experimental methods for eddy current probe design and testing, in: "Review of Progress in Nondestructive Evaluation 3," D. O. Thompson and D. E. Chimenti, eds., Plenum, New York and London.
- Auld, B. A., Riaziat, M., Jeffries, S., and McFetridge, G., 1984d, Improved probe-flaw interaction modeling, inversion processing, and surface roughness clutter, this volume.
- Bahr, A. J., 1982, System analysis of eddy-current measurements, in: "Review of Progress in Quantitative Nondestructive Evaluation 1," D. O. Thompson and D. E. Chimenti, eds., Plenum, New York and London.
- Bahr, A. J., and Cooley, D. W., 1983, Analysis and design of eddy-current measurement systems, in: "Review of Progress in Quantitative Nondestructive Evaluation 2," D. O. Thompson and D. E. Chimenti, eds., Plenum, New York and London.
- Dodd, C. V., and Deeds, W. E., 1968, Analytical solutions to eddy-current probe-coil problems, *J. Appl. Phys.*, 39:2829.
- Muennemann, F., Auld, B. A., Fortunko, C. M., and Padget, S. A., 1983, Inversion of eddy current signals in a nonuniform probe field, in: "Review of Progress in Quantitative Nondestructive Evaluation 2," D. O. Thompson and D. E. Chimenti, eds., Plenum, New York and London.
- Muennemann, F., Ayter, S., and Auld, B. A., 1984, Computation of eddy current signals and quantitative inversion with realistic probe models, in: "Review of Progress in Quantitative Nondestructive Evaluation 3," D. O. Thompson and D. E. Chimenti, eds., Plenum, New York and London.
- Rummel, W. D., and Rathke, R. A., 1984, Eddy current test samples, probes, and scanning system, in: "Review of Progress in Quantitative Nondestructive Evaluation 3," D. O. Thompson and D. E. Chimenti, eds., Plenum, New York and London.